DETECTION OF C_{60} IN THE PROTOPLANETARY NEBULA IRAS 01005+7910

YONG ZHANG AND SUN KWOK

Department of Physics, University of Hong Kong, Pokfulam, Hong Kong, China; zhangy96@hku.hk, sunkwok@hku.hk

ABSTRACT

We report the first detection of buckminsterfullerene (C_{60}) in a protoplanetary nebula. The vibrational transitions of C_{60} at 7.0, 17.4, and 18.9 μm are detected in the *Spitzer*/Infrared Spectrograph spectrum of IRAS 01005+7910. This detection suggests that fullerenes are formed shortly after the asymptotic giant branch but before the planetary nebulae stage. A comparison with the observations of C_{60} in other sources is made and the implication for circumstellar chemistry is discussed.

Key words: infrared: stars – stars: AGB and post-AGB – stars: circumstellar matter

Online-only material: color figures

1. INTRODUCTION

Fullerenes, together with other forms of carbon such as graphite, diamonds, and carbynes, are expected to be the important components of the interstellar medium (Henning & Salama 1998). The most stable fullerene is buckminsterfullerene (C_{60}) which has a soccer-ball-like structure (Kroto et al. 1985). Fullerenes have been proposed as possible carriers of diffuse interstellar bands (e.g., Kroto et al. 1985; Léger et al. 1988), the origin of which is a long-standing mystery (see Herbig 1995, for a review). Foing & Ehrenfreund (1994) found that the laboratory spectrum of C_{60}^{+} in argon and neon matrices shows approximate matches with two diffuse interstellar bands in the near-infrared spectra of stars. Possible formation processes of fullerenes in space that have previously been discussed include condensation in supernova gas, shock-induced decomposition of hydrogenated amorphous carbon (HAC) grains, cold interstellar gas-phase chemistry, etc. (See Moutou et al. 1999; Sellgren et al. 2010, and references therein.) The carbon-rich, hydrogen-poor circumstellar envelopes, such as Wolf–Rayet (WR) stars and R Coronae Borealis (RCB) stars, have also been proposed as favorable sites for the synthesis of fullerenes (Cherchneff et al. 2000; Goeres et al. 1992). However, none of these theoretical predictions have been confirmed observationally.

The search for fullerenes in space started soon after their synthesis in the laboratory. The early efforts to search for the electronic transitions of C_{60} in the optical and UV wavelengths have resulted in no definite evidence showing its presence in space (e.g., Snow & Seab 1989; Herbig 2000; Sassara et al. 2001). Another approach is to search for the infrared vibrational modes of the molecule (Clayton et al. 1995). Kwok et al. (1999) noted a faint feature at 17.85 and 18.90 μm in the *Infrared Space Observatory*-Short Wavelength Spectrometer (ISO-SWS) spectrum of the protoplanetary nebula (PPN) IRAS 07134+1005 and suggested that they could correspond to the ν_{27} and ν_{28} vibrational modes of the C_{60} molecule. However, these features are not confirmed by subsequent *Spitzer* observations. A search of these bands in the reflection nebula NGC 7023 with *ISO* was also not successful (Moutou et al. 1999). Only very recently, C_{60} was unambiguously detected in the planetary nebula (PN) Tc 1 (Cami et al. 2010) and the reflection nebulae NGC 7023 and NGC 2023 (Sellgren et al. 2010). This was followed by the detections of C_{60} in four more PNs (García-Hernández et al. 2010).

These detections of C_{60} in objects at the late stages of stellar evolution raise the concrete question of how C_{60} is formed in a circumstellar environment. Since the element C is synthesized in asymptotic giant branch (AGB) stars and many C-based molecules have been detected in the outflow of AGB stars, it is reasonable to expect that the C_{60} can also be one of the products of circumstellar molecular synthesis. Laboratory results show that the formation efficiency of fullerenes depends on the content of hydrogen, and this has led to the suggestion by Cami et al. (2010) that under a hydrogen-poor environment, the formation of C_{60} is favored, and otherwise the chemical pathway favors the formation of polycyclic aromatic hydrocarbon (PAH) molecules. This scenario is supported by the fact that the infrared spectrum of Tc 1 does not exhibit the aromatic infrared bands (AIBs) commonly assigned as arising from PAH molecules. However, contrary to this scenario, C_{60} was detected in hydrogen-containing PNs showing the AIBs (García-Hernández et al. 2010). The detection of C_{60} in NGC 7023 (Sellgren et al. 2010), an object with strong AIB emissions, also confirms that C_{60} and the AIB carriers can coexist. As an alternative explanation, García-Hernández et al. (2010) suggested that both PAH molecules and fullerenes are formed from the destruction of HAC, and the non-detection of AIBs in Tc 1 is due to the longer survival time of C_{60} molecules. A search for C_{60} in a large sample of RCB stars was performed by García-Hernández et al. (2011). C_{60} is clearly detected in one of the RCB stars showing AIBs, but C_{60} is absent in the most hydrogen-poor ones. These results further support the premise that fullerene and the carrier of the AIBs can coexist.

PPNs are the descendants of the AGB stars and the immediate precursors of PNs (Kwok 1993). The changes of infrared spectroscopic properties in AGB stars, PPNs, and PNs have been known as a consequence of evolution (Kwok 2004). Thus, PPNs can provide a unique opportunity of investigating the formation history of C_{60} in circumstellar envelopes. We have obtained infrared spectra of a sample of PPNs (Zhang et al. 2010) which cover the wavelengths of four C_{60} vibrational transitions at 7.0 (ν_{25}), 8.5 (ν_{26}), 17.4 (ν_{27}), and 18.9 μm (ν_{28}; Nemes et al. 1994). These spectra therefore can serve as a platform to search for C_{60} in PPNs.

In this paper, we report a new detection of C_{60} in a PPN, IRAS 01005+7910. Unlike the other sources in our sample, IRAS 01005+7910 does not show the 21 μm feature and its central star has a higher temperature ($\sim$21,500 K), suggesting

that it is a PPN about to enter the PN stage (Zhang et al. 2010). Hu (2002) classified it as a B2 Ie star with V magnitude of 10.85. Its hydrogen Balmer lines show P Cygni profiles. Through a study of the high-resolution spectrum, Klochkova et al. (2002) concluded that it is a carbon-rich PPN with a luminosity $\log(L/L_{\odot}) = 3.6$ at a distance about 3 kpc.

2. DATA

The study makes use of the infrared spectra retrieved from the Spitzer Heritage Archive (SHA).[1] The observations were conducted with the Infrared Spectrograph (IRS; Houck et al. 2004) on the *Spitzer Space Telescope* (*Spitzer*; Werner et al. 2004) in 2004 and 2006. We have carried out a systematic search for C_{60} in the 10 PPNs studied by Zhang et al. (2010) and found that among the studied sample IRAS 01005+7910 is unique in clearly exhibiting the C_{60} features. The spectra of IRAS 01005+7910 were obtained with the short-wavelength low-resolution module (SL; 5–14.5 μm) as part of the program 30036 (PI: G. Fazio), and the short-wavelength high-resolution module (SH; 9.5–19.5 μm) as part of the program 93 (PI: D. Cruikshank). Details of the data processing have been described elsewhere (e.g., Hrivnak et al. 2009; Cerrigone et al. 2009) and are not repeated here. However, no observation utilizing long-wavelength high-resolution module (LH; 18.7–37.2 μm) was made for IRAS 01005+7910.

3. RESULTS

Figure 1 shows that the *Spitzer*/IRS spectrum of IRAS 01005+7910 is dominated by a thermal dust continuum, the 11.5 μm SiC emission, the AIBs at 6.2, 7.7–7.9, 8.6, 11.3, and 12.7 μm, and the 15–20 μm plateau feature. The AIB and the broad plateau emission features have been previously detected and discussed by Cerrigone et al. (2009) and Zhang et al. (2010). In this paper, we report the detection of the C_{60} features at 7.04 ± 0.05, 17.4 ± 0.05, and 18.9 ± 0.04 μm. The fourth expected C_{60} feature at the 8.5 μm feature is badly blended with the AIB 8.6 μm feature. These C_{60} features have a width of 0.31 ± 0.05 μm, much broader than the spectral resolution. The measured widths of the C_{60} features are similar to those seen in other PNs (see Table 1, García-Hernández et al. 2010). These C_{60} features are not found in any other PPNs in our sample. This suggests that these features likely share a common origin, and thus strengthens the identification of C_{60} as their carrier.

The continuum was fitted, using the feature-free spectral regions, and was subtracted from the observed spectrum. As the features in PPN spectra are usually broad and blended with each other, we conducted a spectral decomposition using the IDL package PAHFIT developed by Smith et al. (2007) in order to accurately measure the feature fluxes. Drude profiles are assumed for the AIBs and C_{60} features. The actual profile of the 15–20 μm plateau, where C_{60} 17.4 and 18.9 μm features are superimposed, is poorly known. We have assumed two broad Gaussian profiles having a width of 1.3 μm and peaked at 16.1 and 17.5 μm for the plateau. (This causes only slight uncertainty in the flux measurements since the C_{60} features are much narrower than the plateau.) For the fitting, we have taken into account the AIBs at 6.2, 6.4, 6.6, 6.8, 7.4, 7.6, 7.9, 8.3, 8.6, and 16.5 μm. Figures 2 and 3 give the zoom-in view of these C_{60} features and the fitting results. From the fitting results, we derived fluxes of $(3.0 \pm 0.3) \times 10^{-15}$ W m^{-2},
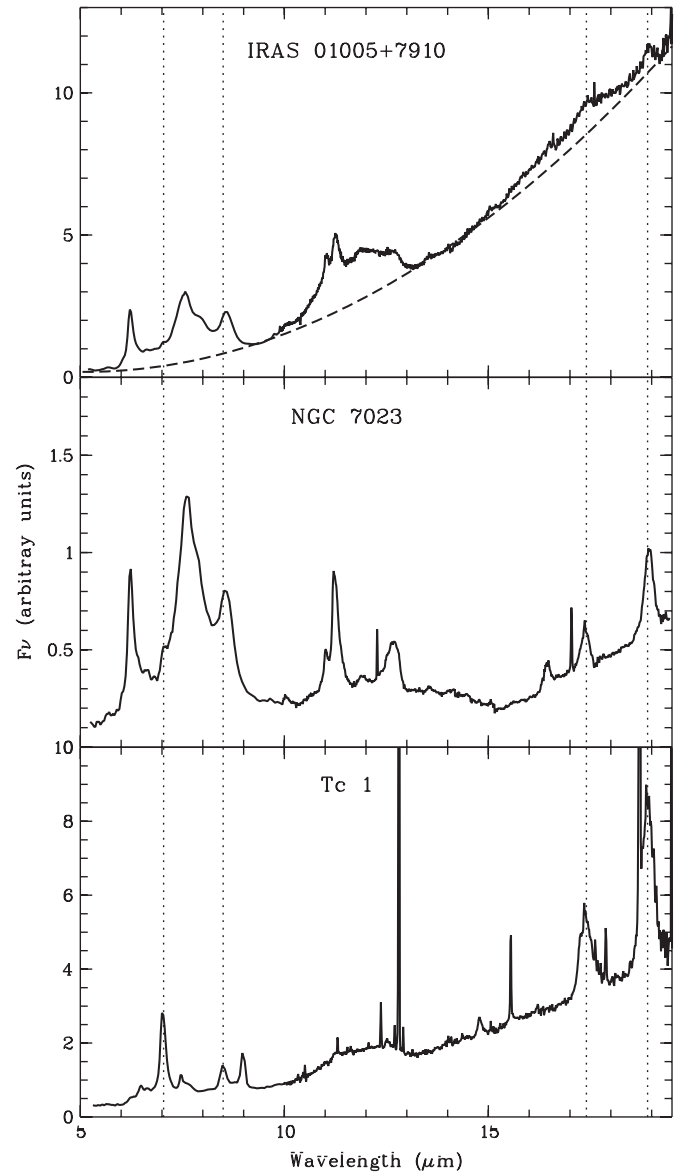
Figure 1. *Spitzer*/IRS spectrum of IRAS 01005+7910 compared to the IRS spectra of two other known C_{60} sources (NGC 7023 from Sellgren et al. 2010 and Tc 1 from Cami et al. 2010). The vertical dotted lines mark the wavelengths of the C_{60} lines at 7.0, 8.5, 17.4, and 18.9 μm. The dashed line represents a fit to the continuum. The other prominent features at 6.2, 7.7, 8.6, 11.3, and 12.7 μm are AIBs.

$(1.2 \pm 0.5) \times 10^{-15}$ W m^{-2}, and $(2.9 \pm 0.5) \times 10^{-15}$ W m^{-2} for the C_{60} 7.0, 17.4, and 18.9 μm features, respectively. The errors of the fluxes were estimated using the full covariance matrix of the least-squares parameters. Sellgren et al. (2010) found that the C_{60} 17.4 μm transition in the spectrum of NGC 7023 is partially blended with an AIB feature. If this is also the case for IRAS 01005+7910, the estimated strength of the 17.4 μm feature would be the upper limit.

Hrivnak et al. (2000) presented the *ISO*-SWS spectrum of IRAS 01005+7910 covering a wavelength range of 2.4–45.4 μm. Due to the lower sensitivity of the *ISO*-SWS compared to the IRS, the C_{60} features are completely overwhelmed by the noise in the *ISO* spectrum. However, a strong feature at 30 μm is detected by *ISO*, and its presence was subsequently confirmed by the *Spitzer*/IRS spectrum (Cerrigone et al. 2009; Zhang et al. 2010). This seems to support the finding by García-Hernández et al. (2010) that all the C_{60} sources exhibit the 30 μm
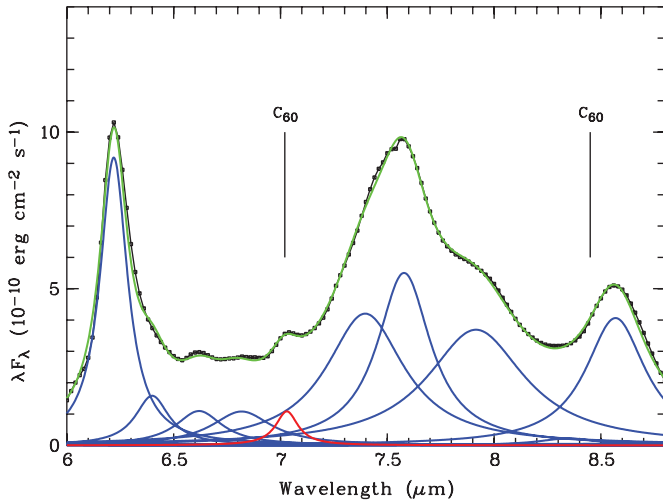
Figure 2. Continuum-subtracted *Spitzer*/IRS spectrum of IRAS 01005+7910 (black dots) between 6 and 8.8 μm. The expected positions of the C_{60} features at 7.04 and 8.45 μm are marked. The blue curves show the model fits to the individual AIBs (a list of the features is given in the text), with the total model spectrum given as the green curve. The red curve is a model fit to the 7.0 μm C_{60} feature. The 8.5 μm C_{60} line is badly blended with the 8.6 μm AIB feature and is not detected.

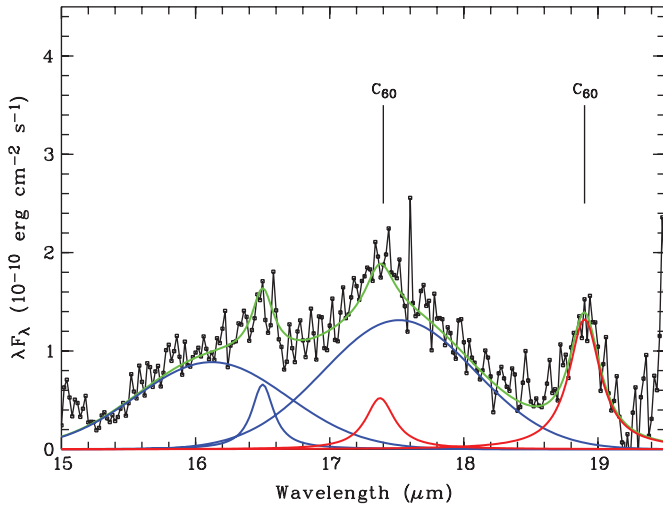(A color version of this figure is available in the online journal.)

Figure 3. Continuum-subtracted *Spitzer*/IRS spectrum of IRAS 01005+7910 (black curve) between 15 and 19.5 μm. The positions of the C_{60} lines at 17.4 and 18.9 μm are marked. The blue curves show the model fits to the individual dust/plateau features, the red curves are the model fits to the 17.4 and 18.9 μm C_{60} lines, and the total model spectrum is given by the green line. Note that the 15–20 μm plateau is fitted by two Gaussian profiles.

(A color version of this figure is available in the online journal.)

feature. However, this correlation only applies to circumstellar sources as the *Spitzer* archive spectra of the reflection nebulae NGC 2023 and NGC 7023 (program 40276, PI: K. Sellgren) do not show the 30 μm feature. The 30 μm feature is commonly seen in carbon-rich AGB stars, PPNs, and PNs (Forrest et al. 1981; Volk et al. 2002), and has been attributed to solid magnesium sulfide (MgS; Goebel & Moseley 1985). However, the identification of MgS as the carrier of the 30 μm feature is debatable as this feature is only detected in carbon-rich sources. Recently, Zhang et al. (2009) found that the MgS dust mass in circumstellar envelopes is not enough to account for the observed feature strength. Therefore, carbonaceous compounds might be more likely to be the carrier of the 30 μm feature.
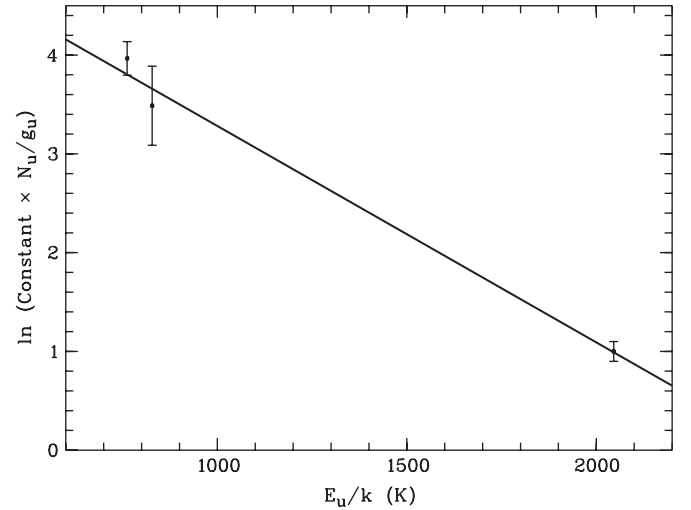

Figure 4. Vibration diagram for the detected C_{60} bands in IRAS 01005+7910. N_u, g_u, and E_u are the population, statistical weight, and excitation energy of the upper level, respectively.

In order to establish a connection between the 30 μm feature with the C_{60} features, more C_{60} sources need to be discovered.

In Figure 1, we compare the *Spitzer*/IRS spectra of IRAS 01005+7910 with two other C_{60} sources, NGC 7023 (Sellgren et al. 2010) and Tc 1 (Cami et al. 2010). All three sources have a strong infrared excess, and IRAS 01005+7910 and Tc 1 have a very red (low color temperature) continuum. IRAS 01005+7910 and NGC 7023 show strong AIB features, which are absent in Tc 1. The fact that IRAS 01005+7910 does not show the narrow atomic lines as seen in the spectrum of Tc 1 is consistent with the object being a PPN and its central star is not hot enough to ionize the surround envelope. After subtracting the continuum, we found that the spectral shape of IRAS 01005+7910 is similar to that of NGC 7023. Cami et al. (2010) also detected a few weaker C_{70} features in Tc 1, which are not seen in IRAS 01005+7910 and NGC 7023. Assuming that all the sources have the same C_{70}/C_{60} strength ratio, the C_{70} features in IRAS 01005+7910 should be well below the detection limit.

4. DISCUSSION

The relative intensities of the C_{60} lines reflect the excitation conditions of the molecule. Assuming a thermal distribution of the vibrational states, Cami et al. (2010) determined the excitation temperature of Tc 1 to be ∼330 K, and suggested that the C_{60} molecules are in a solid state. Similar temperature values were also derived in the PNs studied by García-Hernández et al. (2010). Using a similar procedure as Cami et al. (2010) and García-Hernández et al. (2010), we have constructed a vibrational diagram for IRAS 01005+7910 from the observed fluxes of the three C_{60} lines (Figure 4). An excitation temperature of 460 ± 50 K is derived.

The C_{60} line ratios in IRAS 01005+7910 are $I_{7.0}/I_{18.9} = 1.0 \pm 0.3$ and $I_{17.4}/I_{18.9} = 0.4 \pm 0.2$, which are very close to the values found by Sellgren et al. (2010) in NGC 7023 ($I_{7.0}/I_{18.9} = 0.82 \pm 0.12$ and $I_{17.4}/I_{18.9} = 0.42 \pm 0.02$). Since the central star of IRAS 01005+7910 has a similar temperature as NGC 7023 (∼17,000 K), it is possible that the C_{60} molecules in IRAS 01005+7910 and NGC 7023 are excited in a similar manner. Sellgren et al. (2010) suggest that C_{60} molecules in

NGC 7023 are in the gas phase and they are excited by UV photons from the central star followed by radiative cascade. If this is also the case for IRAS 01005+7910, then the excitation temperature derived above is just a representation of population distribution and is not related to other physical quantities such as kinetic temperature of the gas.

Laboratory measurements show that the wavelengths of gas-phase C_{60} bands shift with temperature (Frum et al. 1991; Nemes et al. 1994). The positions of the four infrared bands ν_{25}, ν_{26}, ν_{27}, and ν_{28} shifts from 6.97, 8.40, 17.41, and 18.82 at 0 K to 7.11, 8.55, 17.53, and 18.97 at 1000 K, respectively. Our measurements show that the wavelengths of all C_{60} bands in IRAS 01005+7910 lie inside these ranges. Assuming that the frequencies of the C_{60} bands have a linear dependence on the temperature, we can estimate the temperature as 100–600 K. The observed widths of the C_{60} features are about 0.3 μm (see Section 3), which correspond to a wavenumber width of $\sim$60 cm^{-1} and $\sim$10 cm^{-1} for the 7 and 17.4/18.9 μm bands, respectively. These values can be compared with the laboratory measured widths of about $\sim$13 cm^{-1} of gas phase C_{60} (Frum et al. 1991), suggesting that a gas-phase origin of the molecule cannot be ruled out.

We estimate the abundance of C_{60} following the same method of Sellgren et al. (2010) by calculating the total strength ratios between the C_{60} and AIB features and assuming that the carrier of the AIB features to contain 6% $\pm$ 2% of interstellar carbon (Cerrigone et al. 2009). The strength ratio of C_{60} to AIB emission is 0.01 in the observed wavelength range of IRAS 01005+7910, resulting in a percentage of carbon in C_{60} of 0.06 $\pm$ 0.02%. This value is slightly lower than those obtained in NGC 7023 (Sellgren et al. 2010) and the PN SMP SMC 16 (García-Hernández et al. 2010), but a factor of 25 lower than that of Tc 1 estimated by Cami et al. (2010).

With the detection of C_{60} in circumstellar envelopes, the next question is how they are formed. In the laboratory, C_{60} can be effectively produced from the vaporization of graphite in a hydrogen-poor environment. Cami et al. (2010) proposed that fullerenes are produced only in hydrogen-poor envelopes created by a late AGB thermal pulse. However, García-Hernández et al. (2010) argued that C_{60} can be synthesized under hydrogen-containing environment. As shown in Figure 1, the spectrum of IRAS 01005+7910 exhibits both hydrogen-containing AIBs and C_{60} features, supporting the latter hypothesis. García-Hernández et al. (2010) also suggested that both C_{60} and PAHs are the products of decomposition of HACs. In this scenario, photochemical processing can lead to dehydrogenation of the dust grains and form PAHs and C_{60} molecules (Scott et al. 1997). On the other hand, the dehydrogenation of dust grains can also induce the formation of H_2 in the grain surfaces (e.g., Fleming et al. 2010). The strongest H_2 line in the observed wavelength range is the 0–0 S(0) transition at 28 μm. This line is not detected in the spectrum of IRAS 01005+7910 (Hrivnak et al. 2000; Cerrigone et al. 2009; Zhang et al. 2010). Moreover, we have detected H_2 in two PPNs with no detectable C_{60} (Zhang et al. 2010). Because of this lack of correlation between the presence of H_2 and C_{60}, we are unable to give additional support for the idea that the formation of C_{60} is the result of dehydrogenation of HACs.

Our detection suggests that fullerenes can be formed in the PPN stage. So far, there is no definite detection of C_{60} in AGB stars. Although Clayton et al. (1995) noted a possible emission feature centered at 8.6 μm in the spectrum of the bright AGB star IRC+10216, the other C_{60} features were not detected in the *ISO*-SWS spectrum (Cernicharo et al. 1999). The circumstellar

spectra of AGB stars are dominated by silicates or silicon carbide emission features (Kwok et al. 1997). Although there are a small number of AGB stars exhibiting AIBs, the AIBs mainly emerge in the post-AGB phase. Is it possible that the formation of C_{60} is related to the emergence of the AIB features? Sellgren et al. (2010) found that the C_{60} and AIB emissions in NGC 7023 have different spatial distributions and attributed this to the effect of UV excitation. It can be argued that the C_{60} and the AIB carriers are already present in the AGB phase of evolution but are not excited until the stars evolve to the PPN phase. However, comparisons between the spectra of AGB stars, PPNs, and PNs suggest a sequence of molecular synthesis, with acetylenes forming in the late AGB phase, leading to the formation of diacetylenes, triacetylenes, and benzene in the PPN phase (Kwok 2004). Since these molecules are detected in absorption, the question of excitation does not arise. Since benzene is the first step toward the synthesis of aromatic materials, we can say with confidence that aromatic compounds only form after the AGB. If C_{60} molecules are synthesized during the AGB, they should be detectable with absorption spectroscopy.

5. CONCLUSIONS

The detection of C_{60} in a PPN as reported in this paper, together with the detection of this molecule in five PNs, confirms that the late stages of stellar evolution is a phase of active molecular synthesis. Beginning with simple diatomic molecules, such as CO, CN, and C_2, dozens of gas-phase organic molecules have been seen in the stellar winds from AGB stars. The formation of acetylene during the late AGB phase is believed to lead to the formation of benzene in the post-AGB phase of evolution. This also coincides with the first detection of vibrational modes of aromatic and aliphatic compounds. From this study, we now learn that gas-phase C_{60} molecules may also form during the same epoch. As the number of C_{60} detection increases, we would be in better position to study the relationships between C_{60} and the carriers of other spectral features, such as the AIBs, and 21 and 30 μm features.

The detection of C_{60} in the outflows from evolved stars also raises the possibility of the molecule being detected in the diffuse interstellar medium as the molecule is stable and should be able to survive journeys through the interstellar medium (Foing & Ehrenfreund 1994). The fact that a large variety of presolar grains (e.g., SiC) have been detected in meteorites (Zinner 1998) raises the possibility that presolar C_{60} can be incorporated into comets and asteroids and be detected in meteorites. In fact, C_{60} and C_{70}, as well as higher fullerenes, have been detected in the Allende meteorite (Becker et al. 1999). The evidence for stellar synthesis of C_{60} in the late stages of stellar evolution as presented in this paper therefore adds further support to the idea of chemical enrichment of the Solar System by stellar molecular products.

REFERENCES

Becker, L., Bunch, T. E., & Allamandola, L. J. 1999, Nature, 400, 6741
Cami, J., Bernard-Salas, J., Peeters, E., & Malek, S. E. 2010, Science, 329, 1180
Cernicharo, J., Yamamura, I., González-Alfonso, E., de Jong, T., Heras, A., Escribano, R., & Ortigoso, J. 1999, ApJ, 526, L41
Cerrigone, L., Hora, J. L., Umana, G., & Trigilio, C. 2009, ApJ, 703, 585
Cherchneff, I., Le Teuff, Y. H., Williams, P. M., & Tielens, A. G. G. M. 2000, A&A, 357, 572
Clayton, G. C., Kelly, D. M., Lacy, J. H., Little-Marenin, I. R., Feldman, P. A., & Bernath, P. F. 1995, AJ, 109, 2096
Fleming, B., France, K., Lupu, R. E., & McCandiss, S. R. 2010, ApJ, 725, 159
Foing, B. H., & Ehrenfreund, P. 1994, Nature, 369, 296
Forrest, W. J., Houck, J. R., & McCarthy, J. F. 1981, ApJ, 248, 195
Frum, C. I., Engleman, R. J., Heddericha, H. G., Bernath, P. F., Lambb, L. D., & Huffmanb, D. R. 1991, Chem. Phys. Lett., 176, 504
García-Hernández, D. A., Kameswara Rao, N., & Lambert, D. L. 2011, ApJ, in press
García-Hernández, D. A., Manchado, A., García-Lario, P., Stanghellini, L., Villaver, E., Shaw, R. A., Szczerba, R., & Perea-Calderón, J. V. 2010, ApJ, 724, L39
Goebel, J. H., & Moseley, S. H. 1985, ApJ, 290, L35
Goeres, A., & Sedlmayr, E. 1992, A&A, 265, 216
Henning, T., & Salama, F. 1998, Science, 282, 2204
Herbig, G. H. 1995, ARA&A, 33, 19
Herbig, G. H. 2000, ApJ, 542, 334
Houck, J. R., et al. 2004, ApJS, 154, 18
Hrivnak, B. J., Volk, K., & Kwok, S. 2000, ApJ, 535, 275
Hrivnak, B. J., Volk, K., & Kwok, S. 2009, ApJ, 694, 1147
Hu, J.-Y. 2002, Chin. J. Astron. Astrophys., 2, 193
Klochkova, V. G., Yushkin, M. V., Miroshnichenko, A. S., Panchuk, V. E., & Bjorkman, K. S. 2002, A&A, 392, 143
Kroto, H. W., Heath, J. R., Obrien, S. C., Curl, R. F., & Smalley, R. E. 1985, Nature, 318, 162
Kwok, S. 1993, ARA&A, 31, 63
Kwok, S. 2004, Nature, 430, 985
Kwok, S., Volk, K., & Bidelman, W. P. 1997, ApJS, 112, 557
Kwok, S., Volk, S., & Hrivnak, B. J. 1999, A&A, 350, L35
Léger, A., D'Hendecourt, L., Verstraete, L., & Schmidt, W. 1988, A&A, 203, L145
Moutou, C., Sellgren, K., Verstraete, L., & Léger, A. 1999, A&A, 347, 949
Nemes, L., et al. 1994, Chem. Phys. Let., 218, 295
Sassara, A., Zerza, G., Chergui, M., & Leach, S. 2001, ApJS, 135, 263
Scott, A., Duley, W. W., & Pinho, G. P. 1997, ApJ, 489, L193
Sellgren, K., Werner, M. W., Ingalls, J. G., Smith, J. D. T., Carleton, T. M., & Joblin, C. 2010, ApJ, 722, L54
Smith, J. D. T., et al. 2007, ApJ, 656, 770
Snow, T. P., & Seab, C. G. 1989, A&A, 213, 291
Volk, K., Kwok, S., Hrivnak, B. J., & Szczerba, R. 2002, ApJ, 567, 412
Werner, M., et al. 2004, ApJS, 154, 1
Zhang, K., Jiang, B. W., & Li, A. 2009, ApJ, 702, 680
Zhang, Y., Kwok, S., & Hrivnak, B. J. 2010, ApJ, 725, 990
Zinner, E. 1998, Annu. Rev. Earth Planet. Sci., 26, 147